Supplementary Information

Two mutations commonly associated with daptomycin resistance in *Enterococcus faecium* LiaS^{T120A} and LiaR^{W73C} appear to function epistatically in LiaFSR signaling

Authors: Milya Davlieva[1], Chelsea Wu[1], Yue Zhou[1], Cesar A Arias[2-6], Yousif Shamoo *[1]

[1]Department of Biosciences, Rice University, Houston, TX 77005 USA; [2]Core for Biomolecular Structure and Function, Department of Genomic Medicine, The University of Texas MD Anderson Cancer Center, Houston, TX, USA; [3]Center for Antimicrobial Resistance and Microbial Genomics and Division of Infectious Diseases, UTHealth McGovern Medical School, Houston, TX, USA; [4]Department of Microbiology and Molecular Genetics, UTHealth McGovern Medical School, Houston, TX, USA; [5]Center for Infectious Diseases, UTHealth School of Public Health, Houston, TX, USA; [6]Molecular Genetics and Antimicrobial Resistance Unit, International Center for Microbial Genomics, Universidad El Bosque, Bogota, Colombia.

*Address correspondence to Yousif Shamoo. E-mail: Shamoo@rice.edu. Address: 6100 Main Street, Department of BioSciences, Houston, TX 77005, USA.

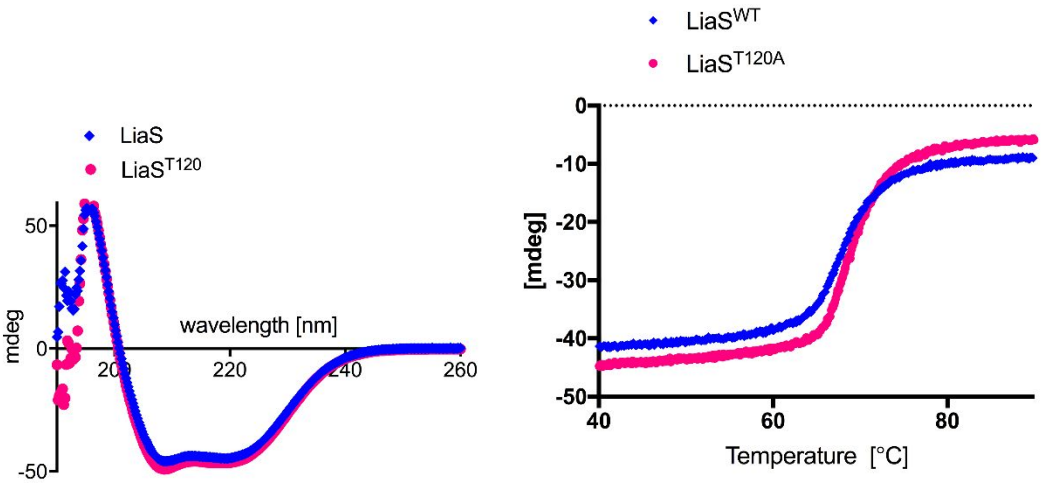

Figure S1. Estimation of secondary structure and folding of *Efm* LiaS and adaptive mutant LiaS^{T120A} cytoplasmic domain (81-355) by circular dichroism (CD). (a) CD experiment suggests that *Efm* LiaS and adaptive mutant LiaS^{T120A} are well folded and have largely alpha-helical secondary structure. Purified LiaS (blue solid line) and LiaS^{T120A} (pink solid line) (b). Thermal stability of *Efm* LiaS (blue) 68.0 ±0.13 °C and adaptive mutant LiaS^{T120A} (pink) 69.15 ± 0.12 °C were determined by changes in CD as a function of temperature (using a JASCO J-815) at 221 nm. Three independent experiments were performed.

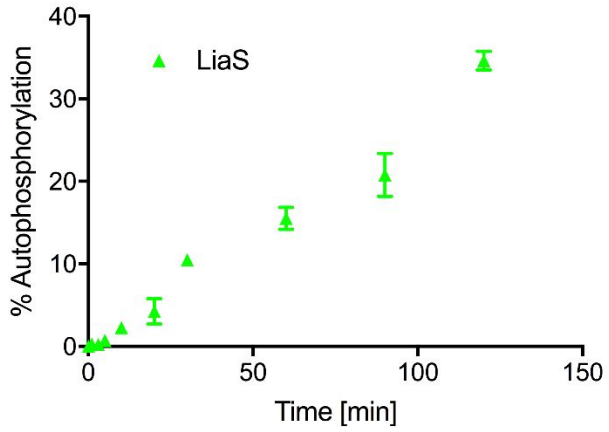

Figure S2. Autokinase activity of the *E. faecium* LiaS (green triangles) was decreased at 25 ºC. Assays were performed in duplicate. The error bars indicate the SD (standard deviation).

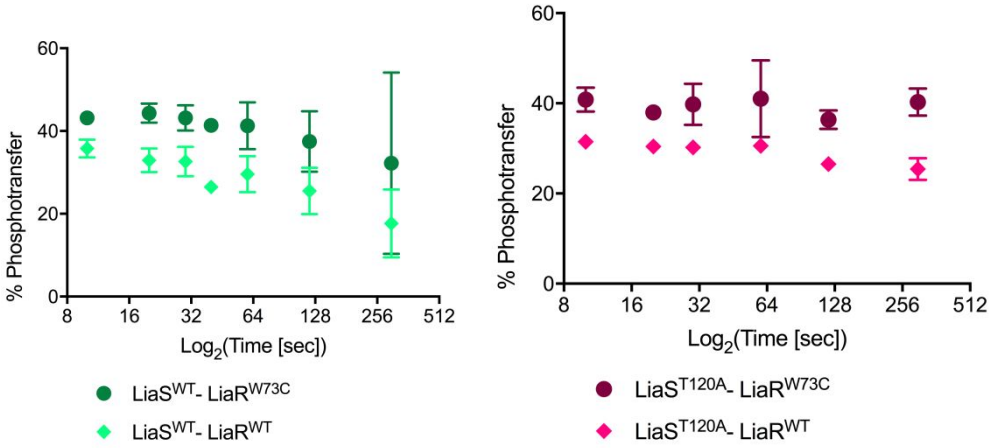

Figure S3. The analysis of the phosphotransfer experiment. The error bars represent the standard deviation. The amount of phosphorylated and non-phosphorylated protein were estimated from the intensity of the upper and lower bands in a phosphogel (Figure 3, main text) using ImageJ[26].

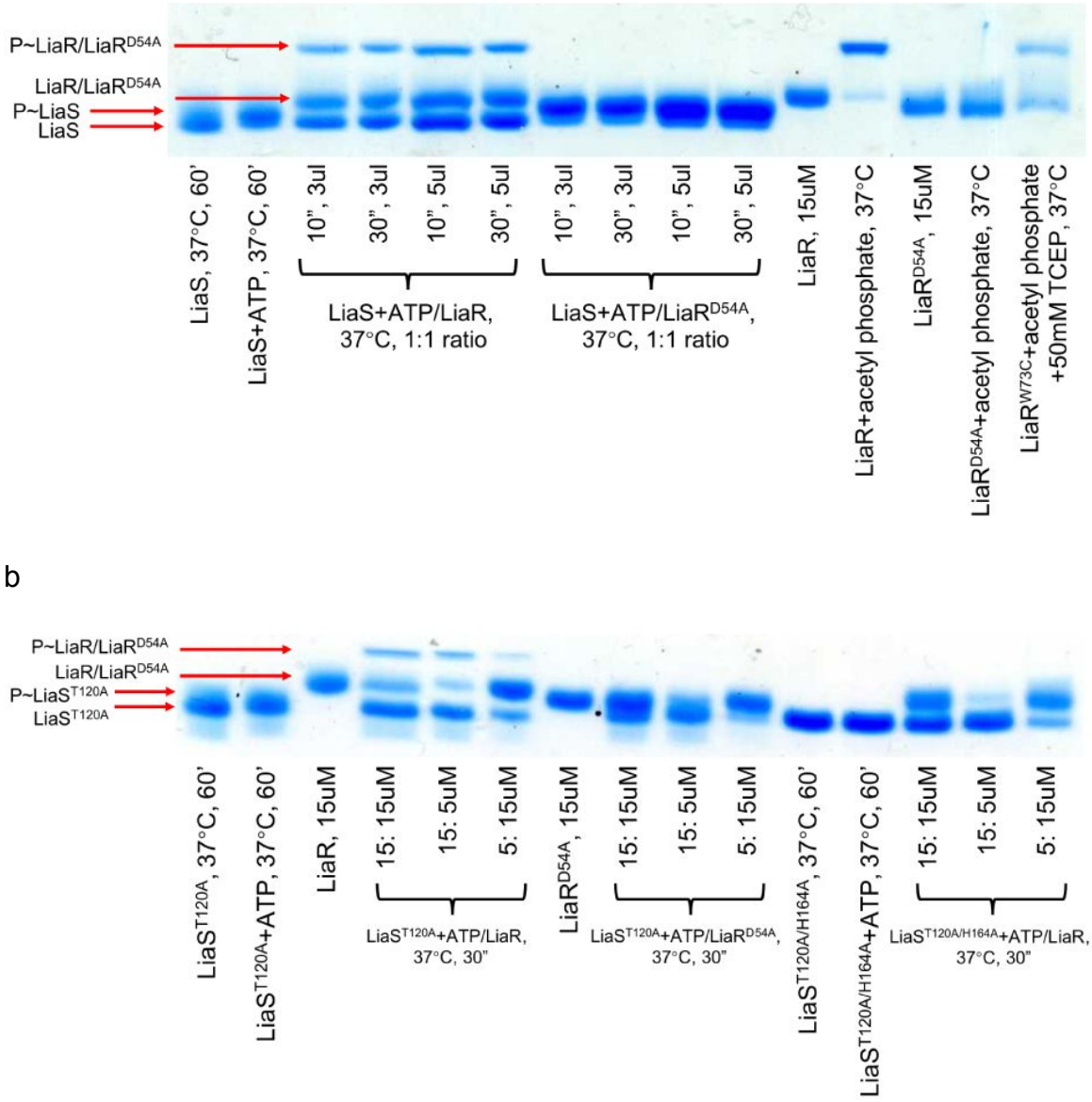

Figure S4. The phosphotransfer reaction from LiaS to LiaR is occurs at Asp-54 of LiaR. (a) LiaR^{D54A} mutant cannot be phosphorylated by LiaS or by the small molecule acetyl phosphate. Different amounts of the reaction (3 and 5 µl) were loaded to show there was no detectable phosphorylated LiaR^{D54A} species. As LiaR^{W73C} introduces a potential disulfide bond, we also show that the addition of the high concentrations of the reducing agent TCEP do not increase the extent of LiaR^{W73C} phosphorylation. Thus, the poor phosphorylation of LiaR^{W73C} is not a consequence of an artifactual disulfide bond. (b)

LiaS^{H164A} mutant cannot phosphorylate LiaR. LiaS^{T120A} was used as a positive control for successful LiaR phosphorylation. LiaS^{T120AH164A} was unable to phosphorylate LiaR or LiaR^{D54A} even at increased stoichiometric ratios.

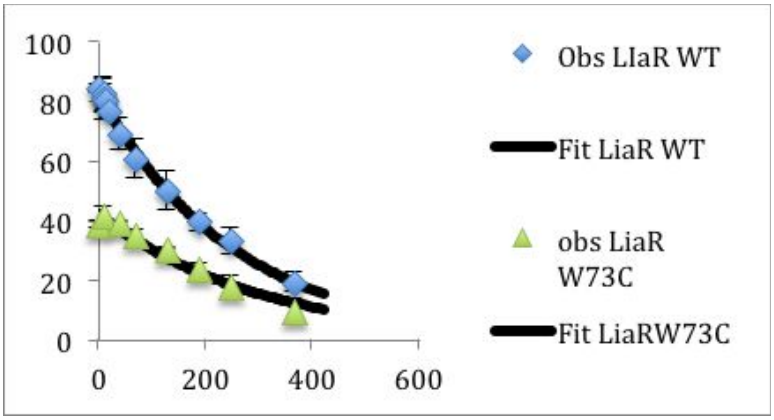

Figure S5. An *in vitro* dephosphorylation assay for the *E. faecium* LiaR has been established. Phosphorylated species were purified using a PD-10 Sephadex G-25M column (GE Healthcare). Reactions were stopped at different time points and samples were subjected to Phos-tag SDS-PAGE electrophoresis. Three independent experiments were performed. The experimental data obtained in Figure 5a (main text) using ImageJ were plotted against incubation time, LiaR (green diamonds) and LiaR^{W73C} (hot pink circles) (Figure 5b) and used to estimate the pseudo-first rates (k, min^{-1}) of dephosphorylation. The error bars were calculated from three independent experiments and represent the standard deviation.